Details of stratification in a sloping bottom boundary layer of Great Meteor Seamount

Hans van Haren

Royal Netherlands Institute for Sea Research (NIOZ), Den Burg, The Netherlands

Received 23 December 2004; revised 3 March 2005; accepted 9 March 2005; published 14 April 2005.

[1] Detailed temperature and current observations show rapid variations in vertical overturning and stratification above Great Meteor Seamount. Classically, steady downwelling interior flow generates a large homogeneous turbulent bottom boundary layer (bbl) and upwelling interior flow generates a small bbl above a sloping bottom. In contrast, the present observations show the dominance of bores and waves in bbl variations above a slope that is non-critical for internal tidal waves. During the upslope tidal phase a small bbl is preceded by a breaking bore extending up to 50 m. The bore shows many small stratified layers. These small layers organize in two large, strongly stratified layers, one at <10 m, the other at ~40 m. During the downslope phase only the lower remains. Above it a thick ~homogeneous layer is observed, which however does not reach the bottom and thus cannot qualify as a bbl having no influence on sediment resuspension. **Citation:** van Haren, H. (2005), Details of stratification in a sloping bottom boundary layer of Great Meteor Seamount, *Geophys. Res. Lett.*, *32*, L07606, doi:10.1029/2004GL022298.

1. Introduction

[2] The frictional boundary layer above a flat bottom in the ocean has a limited vertical extent due to the rotation of the Earth: Ekman dynamics [*Ekman*, 1905]. It holds for steady and oscillatory currents as long as the timescale T of the motion is larger than a couple of hours, $T > \sim 1/f$. Here, $f = 2\Omega\sin\varphi$ denotes the local inertial frequency, which is the normal component of the Earth's angular momentum vector $\mathbf{\Omega}$ at latitude φ. The height of such turbulent bottom boundary layer (bbl) is insensitive to the direction of the current in the interior. When the bottom slopes however, it is sensitive to the alongslope current direction, as was shown for steady flows [*Weatherly and Martin*, 1978] and the consequences of such asymmetrical response for interior ocean mixing and transport have been explored [e.g., *Garrett*, 1990; *MacCready and Rhines*, 1993].

[3] The classic picture is that, on the northern hemisphere, a poleward flow with shallow water to its left generates an upslope Ekman flow. Under stratified interior conditions this flow moves dense water under light water, thereby creating a stable but thin bbl. Consequently, an equatorward flow generates a downslope Ekman flow, which causes an unstable, large bbl. If the interior alongslope flow is steady in direction for more than a few days, the friction is shut down due to a balance between frictional and buoyancy forces [*MacCready and Rhines*, 1993], with a contribution from pressure gradients [*Xing and Davies*, 1999], but the created small- or large bbl remain. The buoyancy force also introduces a bi-directional cross-slope flow [*Phillips et al.*, 1986], with an interior alongslope flow resulting from this flow [*Garrett*, 1990]. However, a steady state is only found for the downwelling case. So far, rather coarse measurements have more or less confirmed varying bbl heights as a function of the interior alongslope flow direction [*Thorpe*, 1987; *Trowbridge and Lentz*, 1991], but subtleties like a bi-directional cross-slope flow are not yet clearly identified in ocean observations, despite some attempts [e.g., *van Haren et al.*, 1994].

[4] In this paper observations of a tidal 'bbl' above Great Meteor Seamount (GMS) show new details of the asymmetric stratification and turbulence above a sloping bottom. Previously, limited current observations off the British continent [*Thorpe*, 1987] and from the Faeroe-Shetland Channel [*Hosegood and van Haren*, 2003] showed bbl varying with tidal periodicity. In the latter turbulence variability was explained following classic Ekman dynamics. Also, bbl asymmetry was found in upslope propagating bores and associated effects on sediment transport having a four-day periodicity [*Hosegood et al.*, 2004].

[5] As the present observations are made in an area dominated by tidal periodicity, with an unpredictably varying response in the bbl, they are also compared with bbl developments by waves on a slope. Laboratory experiments [*Ivey and Nokes*, 1989; *Taylor*, 1993] demonstrated maximum bbl during the upslope wave phase and a minimum during the downslope phase, in contrast with Ekman dynamics. *Slinn and Riley*'s [1996] numerical experiment showed a very thin bbl following a steep front, with most turbulence during downslope (backwash) flow. In all these 2D experiments, a bi-directional cross-slope flow was observed, during up- and downslope phase. Importantly, the bottom slope (9.2–30°) was always critical for the waves used.

2. Instrumentation

[6] A bottomlander was moored near the top of the north-eastern slope of GMS from just after neaps to just before springs (Table 1). The lander held an upward looking 300 kHz, 20° beam angle RDI-Sentinel ADCP storing ensemble averages every 30 s. Its data are transferred to coordinates of cross-slope (u), alongslope (v) and bottom-normal (w) current components, with z = 0 at the bottom.

[7] In the centre of the lander a custom-made thermistor string was attached sampling 128 sensors at 0.5 m intervals at a rate of 1 Hz to an accuracy <0.005°C. Mooring motions were low due to a single ellipsoidal buoy of ~150 kg net buoyancy above the string. Tilt angle at the top of the string

0094-8276/05/2004GL022298$05.00

Table 1. Instrument Details of Bottomlander Moored Between 11/03/2003 10:30 UTC and 16/03/2003 16:00 UTC at 29°59.876′N, 028°18.906′W, 531 m Depth, Bottom Slope ~0.08 (4.7°)[a]

Instrument	Depth [m]	Sampling [s]	#, Increment [m]	Accuracy	Roll, Pitch [°]
NIOZ-2 thermistor string	528.15 (ls)	1	128, 0.5	<0.005°C (0.0015°C noise level)	<4 (top), <3 (top)
RDI 300kHz ADCP	529.75 (fb: 523.2)	30	80, 1.0	u, v:0.01 m s^{-1} w, e:0.003 m s^{-1}	−5.53 ± 0.03, −3.78 ± 0.03

[a]ls = lowest sensor; fb = first bin; # = number of sensors or bins.

was <5°, so that vertical excursions there were <0.3 m. Before and after deployment CTD observations were made near the mooring to calibrate the thermistor string, to establish the large-scale interior density (ρ) stratification expressed in $N = (-g d\ln\rho/dz)^{1/2}$ the buoyancy frequency, with g the acceleration of gravity. The CTD observations are also used to establish the local temperature-potential density anomalies relationship: $\delta\rho_\theta = -0.108 \pm 0.002\ \delta T$ kg m^{-3}, with δT in °C and with salinity also decreasing with depth.

3. Observations

[8] The slope angle of the bottom where the mooring was located near the top of GMS, $\theta \approx 4.5 \pm 0.3°$, is much less than that of most of the mount (10–30°). This θ is still larger than the critical slope α for internal tide gravity wave generation or reflection, which is $|\alpha| = \sin^{-1}[((\sigma^2 - f^2)/(N^2 - \sigma^2))^{0.5}] = 1.6 \pm 0.5° \ll \theta$ for $\sigma = M_2$ and $N = 60 \pm 20$ cpd, the typical local large-scale interior stratification. Nevertheless, the dominant motions show a semidiurnal tidal periodicity through the range of the ADCP (Figure 1). Whether or not these motions represent surface or internal tides, of importance here is the development of the bbl over the tidal cycle.

[9] During each of the ten semidiurnal tidal periods the bbl behaved differently in detail, not associated with the neap-spring change over time. This different development is possibly due to changes in interior stratification and sub-inertial vorticity, thereby affecting the internal wave field and the bottom friction, which also influences barotropic tidal currents. The precise mechanisms for these low-frequency changes are not established. They may be related to atmospheric disturbances and/or topographic waves advecting temperature gradients along the slope. We continue, first discussing the general features of highly asymmetric bbl development, as it holds for all of the tidal cycles.

[10] Towards the end of the down-slope phase at day 73.487 a large ~homogeneous layer is observed extending between 8–25 m, but *not* very close to the bottom (Figure 2). Here, near-homogeneity is determined from the negative temperature gradient, $dT/dz = -2 \pm 1 \cdot 10^{-3}$ °C/10 m, of which the lower bound is close to the adiabatic lapse rate. The above contrasts with the classic view of a large bbl all the way to the bottom. Following Ekman dynamics, the negative alongslope flow should continue to generate a downslope flow, which is only observed above 15–20 m. Below an upslope flow emerges, thereby once (Figure 1, top panel) creating a bi-directional flow commensurate the downwelling steady state in sloping bottom boundary theory [*Garrett*, 1990]. In the example in Figure 2 no such bi-directional flow is observed in this phase. In Figure 2 the transition to up-slope flow is extremely sudden at day 73.489, with a frontal bore of cold water moving up the slope over a range ≥50 m. The upslope flow is to the left and the bore resembles a backward breaking wave. As previously observed in the laboratory [*Taylor*, 1993] and the

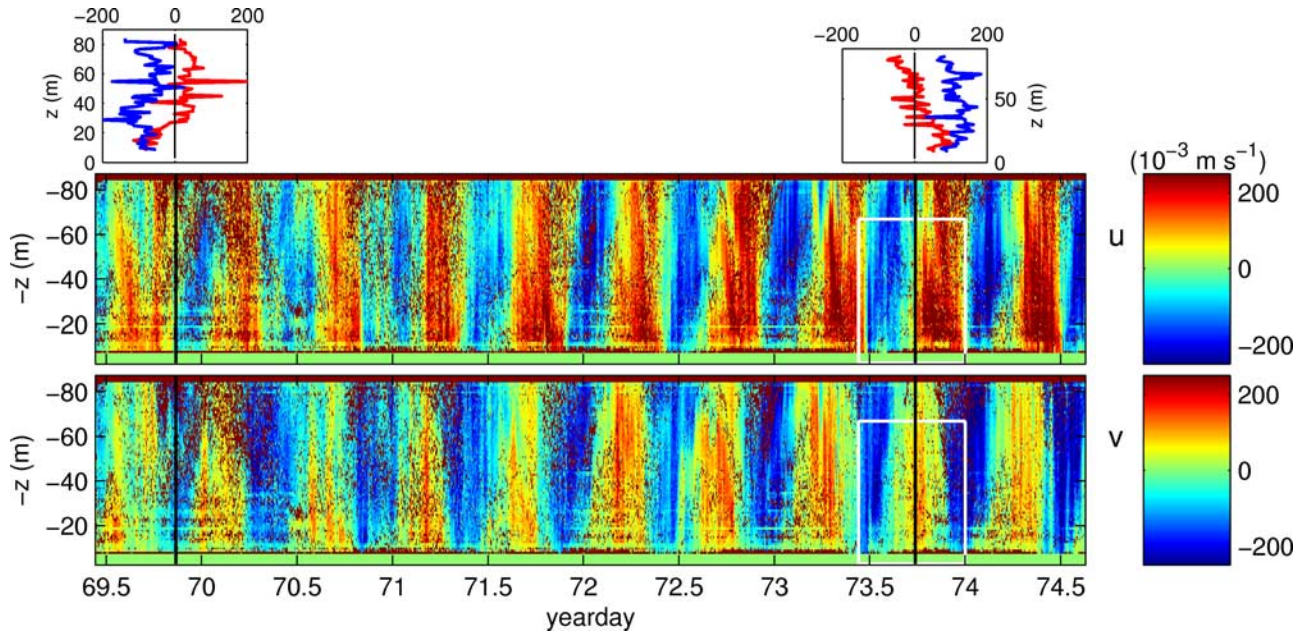

Figure 1. Entire depth-time series of ADCP data u (positive downslope) and v (positive ~poleward). Two examples of bi-directional cross-slope flow (red) are shown in the upper panels with v (blue) at times marked by the black lines. The white rectangle indicates Figure 2.

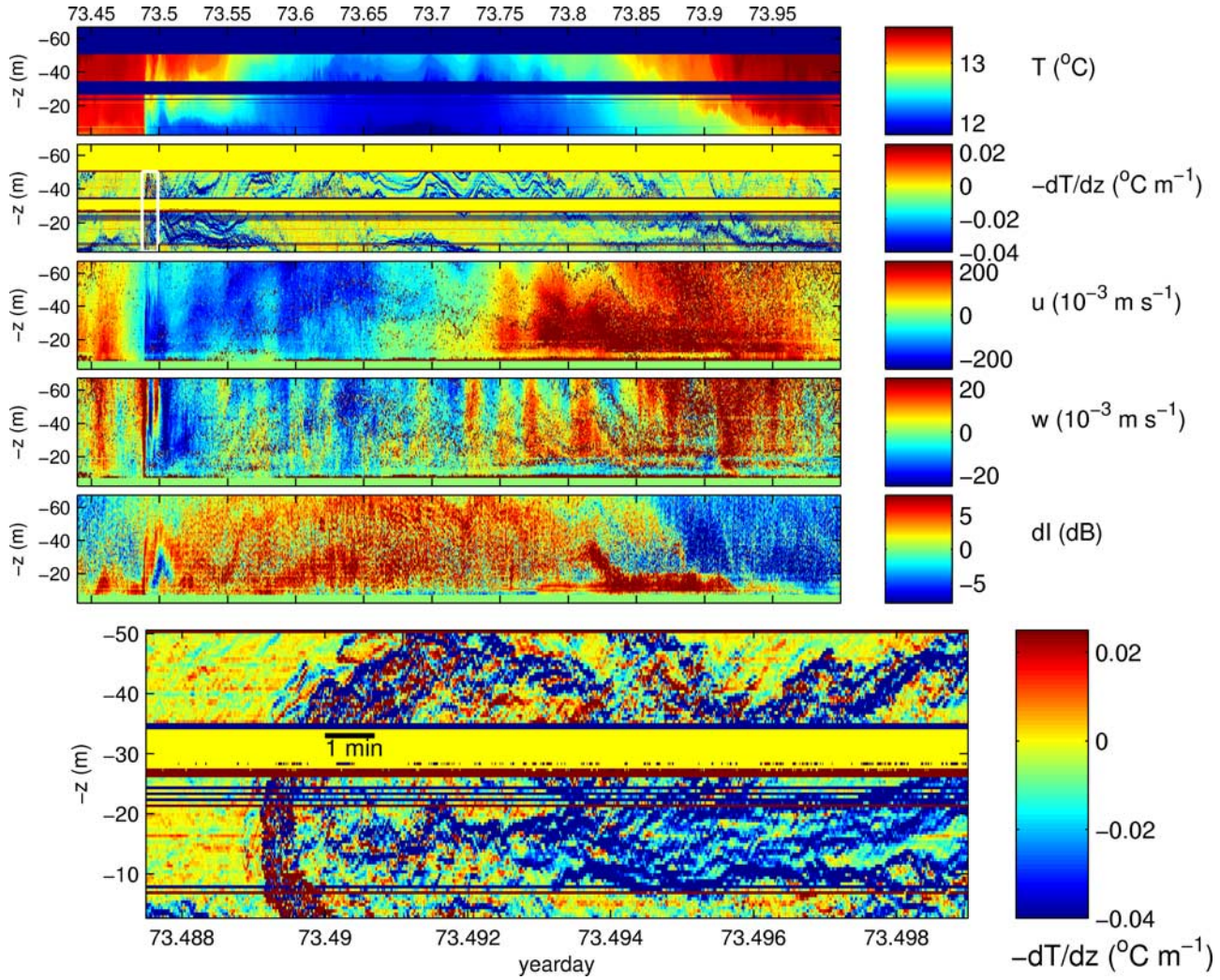

Figure 2. One tidal period of ADCP and thermistor string data. The white rectangle in temperature gradient (dT/dz) indicates the lowest panel, which shows 20 minutes of data of a bore. Bad data in temperature (T) or dT/dz are visible by coloured horizontal bars. A similar bar between 3–7 m indicates 'no data' in ADCP records (cross-slope u, bottom-normal w and relative backscatter dI corrected for water attenuation). Scattered bad data in the ADCP records are brown.

ocean [*Hosegood et al.*, 2004], the bore is accompanied by large w up to 0.1 m s^{-1}, with a relatively large ratio w/u ≈ 0.3. The large w extends from the first ADCP level to more than 80 m. Across this range, which is much larger than in the classic view, the water is briefly highly turbulent, with eddy diffusivity K = $3 \cdot 10^{-4}$–$3 \cdot 10^{-2}$ m^2 s^{-1} estimated over limited vertical ranges using Thorpe scales and evidenced in yellow-red overturns in dT/dz (Figure 2, bottom panel), thereby dominating sediment resuspension (above non-rocky bottom). However, these detailed dT/dz show that less than 5 minutes after the passage of the bore, at day 73.4915, stratification develops in thin (1–2 m thick) layers, mostly between 10–25 m. The streaky pattern of step-like stratification resembles laboratory experiments of mixing in stratified fluids [*McEwan*, 1983], and may be similar to the 'stratification in the bbl' [*Ivey and Nokes*, 1989], although the latter seemed continuous rather than streaky. Continuous stratification was also apparent in *Slinn and Riley*'s [1996] experiments. These differences in layering are difficult to explain quantitatively; the laboratory and numerical experiments were 2D and for critical slope, whilst the present observations are from non-critical tidal slope in a 3D environment.

[11] At day 73.55, wave-like features develop (Figure 2). These resemble solitary waves, but their true solitary wave character depends on the phase speed/frontal speed ratio, which can vary considerably with time [*Hosegood et al.*, 2004]. At day 73.59, the near-bottom stratification (green-blue in dT/dz) seems to vanish, but presumably moves closer to the bottom (<2.95 mab) as it is observed again at day 73.65 without a change in cross-slope current direction. Also, near-bottom water is colder than before, which can only be advected upslope, either locally, or at a nearby site and subsequently advected along the slope (e.g. by tidal waves that have ellipsoidal particle motions in the area). However, it is noted that v ≈ 0.5 u, so that local cross-slope advection seems dominant. Meanwhile, stratified layers that were found at 20 m at day 73.4915 rise to about 40 m at day 73.62, so that a ∼20 m homogeneous (dT/dz < 0) layer is found between the lowest sensor and the stratified layer. The latter supports relatively large and slow waves (30–60 min period; to within a factor of 2 of the local buoyancy

period). These waves are also visible in w. After day 73.55 w does not reach the lowest ADCP level anymore.

[12] U slowly reverses sign from upslope to downslope for the next ~7 hours around day 73.70, first near the bottom (observed at 9 m), where the lower stratified layer is found. The downslope current is far from uniform with height, with maximum amplitude around 30 m and around 70 m some time later. Occasionally in this period a bi-directional u is observed (Figure 1, top right panel), which is not expected to reach a steady state in this phase [*Garrett*, 1990]. Here it is associated with the small-scale internal waves at the interface around 40 m. Below this interface N ≈ 15 cpd, increasing with time in contrast with an expected increasing bbl. The interface at ~40 m at day 73.75 reaches to ~5–10 m at day 73.85–73.9. In the latter period irregular high-frequency internal waves are observed across the entire range having periods of 30–300 s, much less than the buoyancy period of ~30–120 min, and showing occasional overturns. Estimating Thorpe scales gives $K = 4–13 \cdot 10^{-4}$ m^2 s^{-1}. The ADCP's error velocity is substantial (not shown), implying small-scale current inhomogeneities over the beam spread, and the acoustic backscatter drops in value, except near the bottom. The latter may reflect the acoustics of (irregular) interfaces rather than sediment resuspension. These irregular internal motions do not reach the bottom and can therefore not be assigned to a bbl. As a result it does not affect sediment resuspension. The stratification further approaches the bottom, until its closest position just before the arrival of the upslope bore of the next cycle.

4. Summary

[13] The observations from the thermistor string showed some new features of a tidal benthic boundary layer above a sloping ocean bottom. These features are in contrast with an Ekman bbl and resemble a combination of such bbl and a wave bbl. So far, the latter has only been observed in such detail in the laboratory, above critical slopes. The present observations were made above a sloping bottom that was not critical for internal tidal waves using large-scale interior N.

[14] The upslope phase of the tide commences very abruptly, with turbulent overturning extending from 3–50 m. Only during this very brief (<5 min) period a large, truly bbl is formed with associated strong vertical velocities affecting sediment resuspension. This contrasts with the common picture that an upwelling interior Ekman flow imposes a small bbl capped by a stable stratification. Such bbl is formed however, some time after the bore, due to the overturning of breaking wave and associated negative bottom-normal velocity. At this stage a bi-directional cross-slope flow is found with an upwelling interior flow as a result, although only once in the record. Further in time the stratification splits in two layers, one close to the bottom, the other at ~the same height as the maximum bbl during the bore. In between these stratified layers a ~homogeneous layer of 15–30 m is observed. The upper stratification supports high-frequency internal waves, occasionally adopting a solitary wave character. The lower stratification does not support such waves, but it is regularly pushed up and down due to the bottom-normal current.

[15] The Ekman view of the downslope phase is a large bbl. In the present observations no such bbl is found, because of the moderate stratification below the large stratification at ~40 m. This large stratification slowly approaches the bottom, occasionally accompanied by a bi-directional flow associated with the above waves, during a phase of the tide when one would not have expected such cross-slope flow, according to sloping bottom theories. High frequency ≫N irregular 'waves' descend with the stratification, but do not reach the bottom.

[16] In the area, sub-tidal and tidal flows combine or interact: bbl features never showed the same amplitude, duration or position in the water column. This unpredictable behaviour of near-bottom motions strongly affects the variability in mixing and stratification above sloping bottoms, thereby preventing classic shear-induced bbl to resuspend bottom material during most of the tidal cycle. This requires further 3D observational, numerical and laboratory modelling studies.

[17] **Acknowledgments.** I thank the crew of the R.V. Pelagia for deploying the 'mixBB' bottom lander. I enjoyed discussions with Ruud Groenewegen, Martin Laan and Bob Koster during the construction of the NIOZ thermistor string. NWO supported with investment grants 'Oceanographic equipment' and 'LOCO'.

References

Ekman, V. W. (1905), On the influence of the Earth's rotation on ocean-currents, *Ark. Mat. Astron. Fys.*, *2*(11), 1–52.

Garrett, C. (1990), The role of secondary circulation in boundary mixing, *J. Geophys. Res.*, *95*, 3183–3189.

Hosegood, P., and H. van Haren (2003), Ekman-induced turbulence over the continental slope in the Faeroe-Shetland Channel as inferred from spikes in current meter observations, *Deep Sea Res., Part I*, *50*, 657–680.

Hosegood, P., J. Bonnin, and H. van Haren (2004), Solibore-induced sediment resuspension in the Faeroe-Shetland Channel, *Geophys. Res. Lett.*, *31*, L09301, doi:10.1029/2004GL019544.

Ivey, G. N., and R. I. Nokes (1989), Vertical mixing due to the breaking of critical internal waves on sloping boundaries, *J. Fluid Mech.*, *204*, 479–500.

MacCready, P., and P. B. Rhines (1993), Slippery bottom boundary layers on a slope, *J. Phys. Oceanogr.*, *23*, 5–22.

McEwan, A. D. (1983), The kinematics of stratified mixing through wavebreaking, *J. Fluid Mech.*, *128*, 47–57.

Phillips, O. M., J.-H. Shyu, and H. Salmun (1986), An experiment on boundary mixing: Mean circulation and transport rates, *J. Fluid Mech.*, *173*, 473–499.

Slinn, D. N., and J. J. Riley (1996), Turbulent mixing in the oceanic boundary layer caused by internal wave reflection from sloping terrain, *Dyn. Atmos. Oceans*, *24*, 51–62.

Taylor, J. R. (1993), Turbulence and mixing in the boundary layer generated by shoaling internal waves, *Dyn. Atmos. Oceans*, *19*, 233–258.

Thorpe, S. A. (1987), Current and temperature variability on the continental slope, *Philos. Trans. R. Soc. London, Ser. A*, *323*, 471–517.

Trowbridge, J. H., and S. J. Lentz (1991), Asymmetric behavior of an oceanic boundary layer above a sloping bottom, *J. Phys Oceanogr.*, *21*, 1171–1185.

van Haren, H., N. Oakey, and C. Garrett (1994), Measurements of internal wave band eddy fluxes above a sloping bottom, *J. Mar. Res.*, *52*, 909–946.

Weatherly, G. L., and P. J. Martin (1978), On the structure and dynamics of the oceanic bottom boundary layer, *J. Phys. Oceanogr.*, *8*, 557–570.

Xing, J., and A. M. Davies (1999), Processes influencing the circulation and bottom mixing across the shelf slope: The importance of the slope topography and the coast, *J. Mar. Syst.*, *21*, 341–378.

H. van Haren, Royal Netherlands Institute for Sea Research (NIOZ), P.O. Box 59, NL-1790 AB Den Burg, The Netherlands. (hansvh@nioz.nl)